MATERIALS CHEMISTRY FRONTIERS

REVIEW

View Article Online
View Journal | View Issue

Cite this: *Mater. Chem. Front.*, 2023, **7**, 1298

Recent developments in current collectors for lithium metal anodes

Qitao Shi,†[a] Chen Lu,†[b] Yutong Cao,[c] Yufeng Hao,[d] Alicja Bachmatiuk[e] and Mark H. Rümmeli *[afgh]

Received 10th January 2023,
Accepted 11th February 2023

DOI: 10.1039/d3qm00029j

rsc.li/frontiers-materials

Lithium-ion batteries have been widely used in recent decades. However, the anodes being used at present cannot meet the growing demands of the electronics market. Among all the alternative anode materials, lithium is emerging as an advanced anode owing to its high theoretical specific capacity and low operating potential. However, lithium anodes suffer from severe lithium dendrite growth, unstable solid electrolyte interphases, and sluggish kinetics. To address these problems, various strategies have been proposed for the development of practical lithium metal anodes. As reported in previous studies, current collectors play a critical role in facilitating uniform lithium nucleation and deposition, building a stable solid-electrolyte interphase, and improving the dynamics. In this paper, we review the recent developments in current collectors for lithium-ion batteries, retrospect recent research results, and investigate possible future research directions.

1. Introduction

New energy storage systems, such as photovoltaic modules, wind power plants, and hydrogen storage modules, are playing increasingly important roles in modern society.[1] Rechargeable batteries have achieved enormous progress and have acquired broad commercial applications as they act as transfer transportation ports to bridge the gap between clean energy stations and consumer electronics. Currently, several researchers have focused their research attention toward the exploration of secondary batteries with high energy densities. Lithium metal anode (LMA) is considered a promising alternative anode for next-generation lithium-ion batteries (LIBs).[2] Known as a holy grail anode, lithium metal has an extremely high capacity of 3,860 mA h g^{-1}, low density (0.59 g cm^{-3}), and low electrochemical potential, leading to impressive weight and volume energy density.

The first-generation lithium metal batteries (LMB) can be traced back to the 1970s, when Whittingham proposed lithium as an anode and TiS_2 as a cathode.[3] Although Li‖TiS_2 battery exhibited superior energy density and rate capability, the uncontrollable Li deposition triggered thermal runaway and safety hazards. Therefore, research on Li-metal-based secondary batteries was halted. With the development of characterization techniques and growing demand for higher-energy-density devices, a comprehensive understanding of the failure mechanism and relative improvements in Li metal anodes has been proposed. For example, Zhang *et al.* reported that the dendrite would accelerate thermal runaway in a Li‖$LiNi_{0.5}Co_{0.2}Mn_{0.3}O_2$ pouch cell by reducing the self-heating temperature (T_1).[4] Through the generation of the larger solid electrolyte interphase (SEI) and dendritic Li, T_1 would reduce to 72.7 °C after 20 cycles in contrast to 176.1 °C for pristine cells. Moreover, a stable polymer-rich SEI in Li anodes was able to suppress dendrite growth and increase T_1 from 143.2 °C to 174.2 °C.[5] Accelerating rate calorimetry (ARC) and differential scanning calorimetry (DSC) were demonstrated as critical methods in such studies.[6–8] The improved understanding of the failure mechanism in LMAs have once again attracted research interest.

[a] *Soochow Institute for Energy and Materials InnovationS, College of Energy, Key Laboratory of Advanced Carbon Materials and Wearable Energy Technologies of Jiangsu Province, Key Laboratory of Core Technology of High Specific Energy Battery and Key Materials for Petroleum and Chemical Industry, Soochow University, Suzhou 215006, China. E-mail: mhr1@suda.edu.cn, mhr1967@yahoo.com*
[b] *School of Electronic and Information Engineering, Changshu Institute of Technology Changshu 215500, China*
[c] *School of Materials Engineering, Changshu Institute of Technology, Changshu 215500, China*
[d] *National Laboratory of Solid State Microstructures, College of Engineering and Applied Sciences, Jiangsu Key Laboratory of Artificial Functional Materials and Collaborative Innovation Center of Advanced Microstructures, Nanjing University, Nanjing 210023, China*
[e] *LUKASIEWICZ Research Network, PORT Polish Center for Technology Development, Stablowicka 147, Wroclaw 54, Poland*
[f] *Leibniz Institute for Solid State and Materials Research Dresden, P.O. Box 270116, D-01171 Dresden, Germany*
[g] *Centre of Polymer and Carbon Materials, Polish Academy of Sciences, M. Curie-Sklodowskiej 34, 41-819 Zabrze, Poland*
[h] *Institute of Environmental Technology, VSB-Technical University of Ostrava, 17. Listopadu 15, 708 33 Ostrava, Czech Republic*
† These authors contributed equally to this work.

LIBs generally consist of anode and cathode materials to reversibly store lithium, a current collector (CC) to collect electrons, an electrolyte to enable the transportation of lithium ions, and a separator to isolate the anode and the cathode. Battery performance is essentially determined by the Li^+ storage capacity and working voltage of both the anode and cathode materials. 3In addition, the battery configurations, namely the electrolyte, separator, and CC, have a profound impact on the performance as they determine the release capacity of the electrode materials.[9,10]

CCs are used to support the active materials, collect the electrons involved in the electrochemical reaction, deliver the electrons between the electrode materials and the external circuit, and release the thermal heat generated during the electrochemical process.[11–14] A typical CC should be electronically conductive, ionically insulated, electrochemically inactive, mechanically robust, and cost-effective. As the potential at the Li anode side is approximately 0 V, the CC at the Li metal side should not react with lithium or the electrolyte in such a reduction environment. Moreover, the CC must possess high mechanical strength so that it can withstand the stress generated when active materials undergo volume expansion. As a result, copper (Cu) foil was employed as a commercial CC for the anodes.

In LMBs, the mechanism of lithium ion storage on the anode side is quite different from that in LIBs.[15,16] In LIBs, Li^+ undergo electrochemical reactions with the anode materials upon charging, and Li deposition behavior occurs only under fast charging and low-temperature charging. During this process, Li^+ ions do not directly interact with the CCs. In contrast, Li ions are converted to Li metal on the CC *via* electrodeposition in LMBs. Hence, the CC has a remarkable impact on the Li deposition process, including the Li nucleation overpotential, Li plating morphology, and cycle life. Commercial Cu foil is generally used as CC for LIBs but is not adaptive for LMBs because it is weak in guiding lithium plating owing to its lithiophobic nature. Effective approaches such as modification of Cu foil or designing practicable CCs have been proposed to advance the development of lithium anodes. In this review, we introduce the advances in modified Cu foils and three-dimensional (3D) porous Cu structures, investigations on CCs beyond Cu foils, and designs of functional CCs, as illustrated in Fig. 1. Facile modifications of commercial Cu foil are regarded as the most cost-effective approach because they take advantage of the current techniques to produce Cu foil without excess research input. The construction of 3D porous Cu structures can further enable the operation of CCs because they offer free space to withstand the infinite volume change of Li plating. Nickel-based CCs are worth developing because of their abundant resources and low price. Carbon-based CCs provide stronger plasticity and flexibility, and are expected to be applied in flexible electronics. To accelerate the practical process of lithium metal anodes, CCs that can stabilize the SEI and prevent thermal runaway should receive more attention.

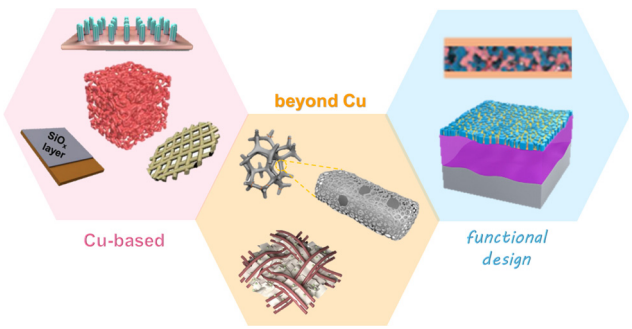

Fig. 1 A schematic illustration of the developments in CCs for lithium metal anodes: Cu-based CCs, CC beyond Cu, and CCs of functional designs.

2. Modifications on Cu foil

The materials of CCs utilized in LIBs include aluminum (Al), copper (Cu), nickel (Ni), stainless steel, and carbon with 2D planar or 3D porous type.[16] Currently, Al and Cu foils are applied as CCs for cathodes and anodes, respectively. Despite its low cost and light weight, Al foil undergoes corrosion at low potential in LIBs, which makes it unfavorable for supporting anode materials.[17] Cu foil has emerged as a commercial anode CC owing to its high conductivity, ductility, and stability at low operating voltages.[18] The widely used commercial Cu foil has a 2D planar structure with a low surface area and is lithiophobic in nature. In a typical LMB system, when Li^+ ions are extracted from cathodes and plated on Cu foil, the deposited lithium suffers from an uncontrollable nucleation and growth process, resulting in an uneven morphology and low coulombic efficiency. Therefore, it is necessary to develop a suitable CC for reversible Li deposition and stripping.

As Cu foil has been commercialized and that the manufacturing technique is relatively mature, modifications to commercial Cu CCs have been extensively regarded as a cost-effective approach for improving the feasibility of LMBs. To address the limitations of bare Cu, incorporating lithiophilic materials and constructing 3D structures are the most common and effective strategies.[19] Huang *et al.* employed a trace amount of Au on Cu foil as the CC to eliminate the uncontrollable Li plating on Cu foil for an anode-free Li_2S-based full battery.[20] A commercial ultrathin-Au film was carefully coated on Cu foil, as shown in Fig. 2a–c. During cycling, Au transformed into a lithophilic Li_xAu alloy as a nucleation site, leading to dendrite-free Li deposits on the Au film. In a $Li_2S\|Cu$ cell, Li is plated parallel to the Cu foil with an area equal to that of the Li_2S cathode, as shown in Fig. 2a. In contrast, the Li deposition area matches well with the location of the Au film in $Li_2S\|Au/Cu$, as shown in Fig. 2b and c, indicating that the diffusion pathway and deposition area of Li can be induced by Au. Consequently, the overpotential (the difference between the lowest transient potential and the steady cycling potential) of Li deposition during the initial process on the Au/Cu CC is approximately 0, while that of the bare Cu foil is 36.8 mV (Fig. 2d and e). In addition, Ag was reported to be able to manipulate the Li deposition behavior in Cu-based CCs in the same manner. Similar Au- and Ag-induced-nucleation designs

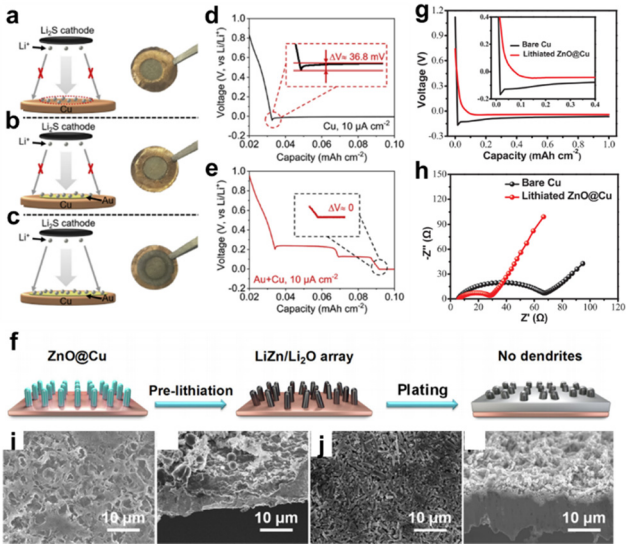

Fig. 2 Metal-based nucleation sites. (a) Schematic configurations and digital photographs of the anodes extracted from: (a) Li_2S‖Cu, (b) Li_2S‖8-Au/Cu, and (c) Li_2S‖12-Au/Cu cells. The photographs of the anodes were taken at fully charged state. Voltage profiles of (d) Li‖Cu and (e) Li‖Au/Cu cell. Reproduced with permission.[20] Copyright 2020 Elsevier B.V. (f) Schematic illustration of Li plating on lithiated ZnO@Cu electrode. (g) Initial voltage profiles of the plating for bare Cu and lithiated ZnO@Cu electrode. (h) EIS of bare Cu and lithiated ZnO@Cu electrodes in Li‖Cu cells after 10 cycles. Top-view and cross-sectional view SEM images of (i) bare Cu and (j) lithiated ZnO@Cu electrodes after 20 cycles. Reproduced with permission.[29] Copyright 2019 Elsevier B.V.

have been reported many times and have achieved great improvements.[21–28]

Compared with noble metals such as Au and Ag, inexpensive metal compounds are preferred for developing high-performance Cu-based CCs. Despite the lithiophobic feature of pure Cu, some copper compounds, such as CuO and Cu_2O, were found to be lithophilic.[30–32] Involving Cu foil as a reactant, a lithiophilic surface could be generated. It has been reported that other metals or metal compounds can also work as nucleation sites, such as Sn,[33] ZnO,[29,34] and Al_2O_3.[35] Xiong *et al.* proposed a lithiated ZnO nanoarray-decorated Cu foil to regulate the Li plating/stripping behavior.[29] The ZnO nanorod arrays were synthesized *in situ* by a solution deposition route. The ZnO nanorods were transformed into LiZn and Li_2O after lithiation. The conductive alloy array enabled a uniform electrical field distribution and even Li-ion flux, which functioned as nucleation sites to guide dendrite-free Li deposition. Fig. 2f illustrates the Li plating process on the lithiated ZnO@Cu electrode. The voltage profiles of the electrodes in Fig. 2g confirm that the overpotential of lithiated ZnO@Cu was lower than that of bare Cu, suggesting the lithiophilic nature of the LiZn/Li_2O arrays. The EIS spectra in Fig. 2h reveal that the charge transfer resistance of lithiated ZnO@Cu is much smaller than that of bare Cu, indicating faster kinetics during cycling. The morphologies of the electrodes after 20 cycles could explain the different performance (Fig. 2i and j). The lithiated ZnO@Cu electrodes maintained a smooth surface, a homogenous thickness and very few dendrites. While the lithiated bare Cu electrodes had a non-uniform surface and a porous microstructure. It can be concluded from the two cases in Fig. 2 that by changing the characteristics of the Cu foil surface from lithiophobic to lithiophilic, a more reversible Li plating/stripping process can be acquired. More recently, Huang *et al.* modified Cu foil with Cu_3N nanowires by an *in situ* method,[36] utilizing alkali to etch and simple thermal annealing to nitride. This work is representative of many studies[30–32] that take full advantage of Cu foil as a reactant to generate a lithiophilic surface.

In addition to the aforementioned metal-based nucleation sites, numerous non-metal chemicals have been proposed as good substrates for inducing Li deposition. Yang *et al.* employed a homogeneous porous SiO_x layer deposited directly over the Cu CC (LI-SiO_x@Cu) as depicted in Fig. 3a.[37] A silicone-based adhesive of the tape was first applied on a fresh Cu foil and converted to SiO_x layer by a commercial infrared laser with working power of 1.5 W for two-time lasing treatment. The voltage profiles shown in Fig. 3b reveal that the nucleation energy barrier of LI-SiO_x@Cu was relatively smaller than that of bare Cu, indicating more favorable nucleation kinetics in LI-SiO_x. The inset in Fig. 3b explains one of the reasons for the enhanced kinetics, namely, the abundant lithiophilic sites produced by LI-SiO_x. In addition, a small amount of laser-induced graphene was visually identified by performing transmission electron microscopy (TEM), which also played a role in accelerating the electrochemical dynamics. The as-prepared LI-SiO_x@Cu suppressed the formation of Li dendrites and inactive Li and presented a higher average CE of 99.3%, demonstrating outstanding performance in LMB with zero excess of lithium. The energy density of the prepared anode-free pouch cell with $LiFePO_4$ as the cathode is ≈209 W h kg^{-1}, which is twice as

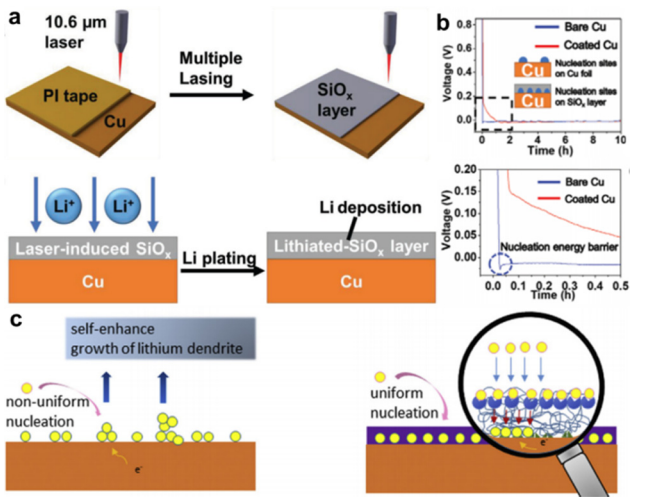

Fig. 3 Non-metal lithiophilic sites. (a) Schematic diagram for the formation of laser induced SiO_x layer on the Cu CC and the lithium plating behavior. (b) Voltage profile of bare Cu and Cu with LI-SiO_x layer. Reproduced with permission.[37] Copyright 2020 Wiley-VCH Verlag GmbH & Co. KGaA, Weinheim. (c) Schematic of the mechanism of PDA-induced Li deposition. Reproduced with permission.[39] Copyright 2019 Elsevier B.V.

high as the commercial $LiFePO_4$ pouch cells. However, the cycling stability and failure mechanism were not discussed. Yang *et al.* prepared a 3D-hierarchical composite material by processing polyimide films on Cu foils with a similar lasing treatment,[38] which consisted of many laser-induced N-doped graphene walls that served as nucleation centers upon Li deposition. Overall, these studies offer a fast, low-cost, and scalable approach to develop modified Cu foils for Li-metal anodes.

Various lithium-reactive materials can be considered as options for nucleation sites to modify Cu foils for advanced LMBs. Organic materials could also be considered as options to protect Cu foil CCs owing to their structural flexibility. Liu *et al.* introduced a functional polydopamine (PDA) layer onto Cu foil to improve Li deposition.[39] The PDA layer was prepared by the polymerization of dopamine in Tris-HCl buffer solution at a reaction temperature of 20–60 °C for 24–48 h. During the first deposition process, Li^+ reacted with poly(5,6-dihydroxyindole) to generate poly(5,6-indolequinone). Subsequently, the carbonyl groups on the PDA layer stored Li^+. Upon subsequent plating, the stored Li^+ is preferentially reduced *in situ* to Li metal. Fig. 3c shows the Li deposition mechanism induced by bare Cu and PDA. As a result, the Li-Cu asymmetric cells showed a high CE of 97% for 100 cycles, and the $LiFePO_4$‖Li@PDA-Cu full cell displayed excellent long-term cycling stability. Hwang *et al.* further modified these PDA-Cu CCs with Ag nanoparticles as nucleation seeds and graphene oxide as an artificial SEI.[27] The modified CC exhibited an improved CE of 98.1% in an asymmetric cell, a high average CE of 98.5% and a high capacity retention of 55.7% after 60 cycles in an anode-free full cell with NMC as the cathode.

Some other organic materials, such as polyvinylidene difluoride,[40] polyethylene oxide,[41] and polyvinyl alcohol,[42] have been investigated as the protection layer for Li metal anodes. These organic material-coated Cu foils not only enable uniform Li deposition/stripping but also help construct a more stable SEI. However, the Li^+ diffusion coefficient is low in organic materials, which probably influences their rate capability.

Recently, numerous 3D CCs have been presented and proven to be an efficient solution to ensuring LMB operating the fast kinetics of LMB operation. These 3D structures can efficiently avoid dendrite growth and volume expansion upon Li plating because of their large surface areas and rapid electron and ion pathways. Nevertheless, the large-scale, cost-effective, and controllable production of 3D structured CCs is still challenging, such as 3D carbon nanotube sponge,[43–45] graphene foam,[46] and nickel foam,[47,48] among others. Thus, it would be valuable to develop 3D structured CCs by employing existing commercial products as general templates.

Zhang *et al.* suggested a scalable route to construct a 3D porous structure on commercial Cu foil *via* a liquid Ga-induced alloying–dealloying procedure, as shown in Fig. 4a.[49] For a typical preparation process, the liquid Ga was uniformly smeared over the surface of the Cu foil and further annealed at 100 °C to form a $CuGa_2$ alloy. After the selective etching of Ga, the residual Cu atoms rearrange into a 3D nanoporous

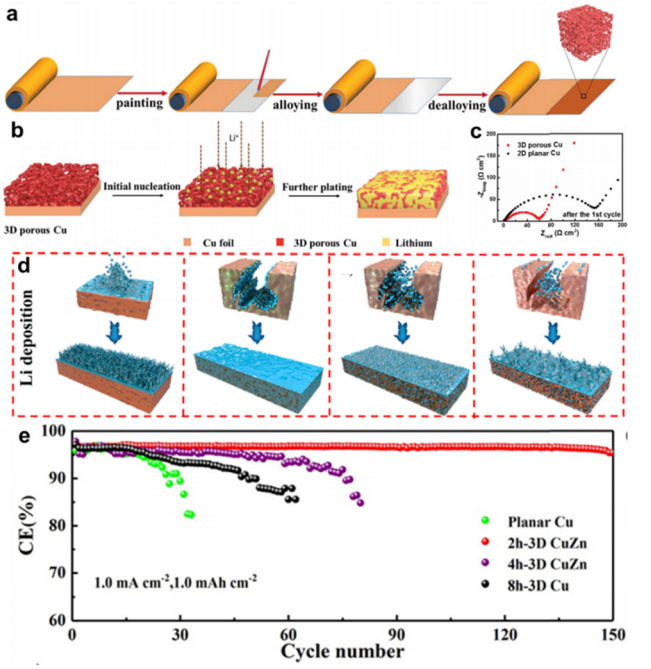

Fig. 4 3D porous structured Cu foil. (a) Schematic illustration showing the preparation process of the 3D porous Cu from 2D planar Cu foil. (b) Schematic illustrations showing the structural changes in 3D porous Cu. (c) EIS spectra of the 2D planar and 3D porous Cu CCs after 1 cycle. Reproduced with permission.[49] Copyright 2019 The Royal Society of Chemistry. (d) Li deposition diagram of different CCs with 0, 2, 4, and 8 h dealloying time. (e) Coulombic efficiency of the different CCs. Reproduced with permission.[50] Copyright 2020 American Chemical Society.

architecture. Fig. 4b shows the structural changes upon initial nucleation and further plating during lithiation in 3D porous Cu. The porous skeleton of 3D Cu possesses numerous charge centers that can build a more uniform electric field, which helps to homogenize the current density and prevent Li dendrite propagation. Fig. 4c shows the internal impedance of different CCs after the initial Li plating/stripping, from which the interfacial resistance of SEI formation (R_{SEI}) and charge transfer resistance (R_{ct}) can be calculated using equivalent circuits. The half-cell with 3D porous Cu exhibited a much lower $R_{SEI} + R_{ct}$ (54.9 Ω) than that of the planar Cu foil (157.9 Ω). Thus, better electrochemical performance was achieved in both symmetrical and full cells.

More commonly, researchers have employed various commercial Cu alloy foils as initial reactants to synthesize 3D porous Cu foils, such as Cu–Zn alloy,[50–52] Cu–Mn alloy,[53] Cu–Sn alloy,[54] and Cu–Zr alloy.[55] Interestingly, foreign metal atoms in the alloy may play a positive role in the induction of Li deposition. Tang *et al.* investigated the role of residual CuZn alloys in a dealloyed CuZn framework using density functional theory (DFT) calculations and *in situ* experiments.[50] A series of dealloyed CuZn frameworks with different etching times (0, 2, 4, and 8 h) were employed as research objects. Fig. 4d shows the Li deposition behavior on different CCs with dealloying times of 0, 2, 4, and 8 h. Li dendrites grew sporadically on 2D planar

Cu, whereas 2h-3D CuZn and 4h-3D CuZn CCs guided Li plating into the inner pores, thus promoting the growth of Li deposits. When fully etching the foreign Zn atoms for 8 h, the deposition surface layer of the residual 8h-3D Cu was smoother than that of 2D planar Cu, but rougher than that of 2h-3D CuZn and 4h-3D CuZn. It can be speculated that the residual 3D CuZn phase reduces the local current density and suppresses the growth of Li dendrites. DFT calculations and *in situ* measurements were conducted to further verify the lithophilicity of the CuZn alloy. With the assistance of the 3D porous skeleton and residual lithiophilic CuZn alloy, 2h-3D CuZn maintained a CE of 95% for 150 cycles, as depicted in Fig. 4e, which was much higher than that of the control sample.

Constructing a 3D structure on a Cu foil base is another popular strategy for the design of porous CCs. Wang *et al.* fabricated a 3D granular piling structure by casting Cu microparticle solution onto Cu foils.[56] The granular piling structure managed to dynamically adapt to volume change during Li plating/stripping to realize quick stress relaxation. More commonly, various works employed a template method along with electrodeposition to create porous structure, for instance, colloidal template method combined with copper electrodeposition,[57–59] porous CoP film produced by electrodeposition,[60] and hydrogen bubble dynamic template method.[61] Moreover, assembly of one-dimensional nanorods, nanofibers, or nanowires were also proposed as an efficient approach to design porous framework, such as ZnO-modified polyacrylonitrile (PAN) fiber,[22] uniform vertically aligned Cu pillars,[55] Sn-coated Cu nanowires,[33] ZnO nanorod arrays,[29] and vertically aligned carbon nanofibers.[62] Generally speaking, the 3D porous structures offer a large surface area to reduce the local current density and Li^+ flux to homogenize the Li deposition, and provide abundant space to accumulate the volume change during lithium plating, resulting in dendrite-free Li anode with enhanced cyclability.

In addition to the 3D porous CCs built on planar Cu foil, some Cu and Cu alloys with inherent 3D frameworks are considered as intact CCs or starting materials to build more effective CCs. Shao *et al.* employed a commercial copper foam (CF) as skeleton to grow vertically aligned hierarchical copper fibers as modified CCs (HCF/CF) for dendrite-free lithium metal anodes.[63] Fig. 5a illustrates the different Li deposition behaviors on the CF and HCF/CF CCs. The numerous Cu fibers acted as charge centers and nucleation sites in the HCF/CF framework, and lithium tended to nucleate and deposit on the copper fibers and then fill the space between the fibers. A homogeneous layer of lithium was eventually deposited on the HCF/CF framework by repeated cycling. In contrast, Li dendrites and dead Li were formed on bare CF CCs. The CEs

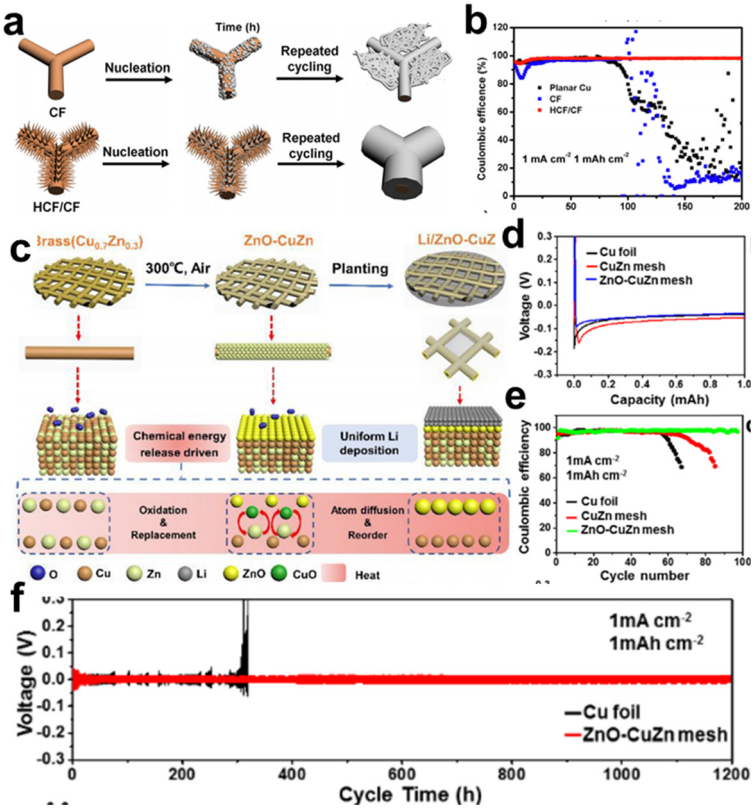

Fig. 5 Cu framework based CCs. (a) Schematic illustration of the Li deposition on the CF and HCF/CF CC. (b) Coulombic efficiencies of Li plating/striping on CF, planar copper, and HCF/CF. Reproduced with permission.[63] Copyright 2019 Elsevier B.V. (c) Schematic of *in situ* formed lithiophilic layer on a commercial 3D brass mesh as a modified CC. (d) Voltage profiles of the Cu foil, CuZn mesh, and ZnO–CuZn mesh. (e) CEs of Li plating/striping on Cu foil, CuZn mesh, and ZnO–CuZn mesh. (f) Voltage curves of the Cu foil and ZnO–CuZn mesh in symmetrical cells. Reproduced with permission.[64] Copyright 2019 American Chemical Society.

for Li plating/stripping on both CCs are shown in Fig. 5b. HCF/CF maintained a high CE of 98% for over 200 cycles, while CF displayed an unstable CE, which dropped to 30% after 130 cycles. Furthermore, the Li@HCF/CF|$LiFePO_4$ (LFP) full cell exhibited capacity retention of 95.6% after 500 cycles.

Ci *et al.* elaborately deposited the Au layer onto one side of the Cu foam by magnetron sputtering.[21] The lithiophilic Au nucleation sites induced lithium metal to grow toward the direction opposite to that of the separator and onto the back surface of the Cu foam. Combined with the unique structure of the Cu foam, the growth direction and morphology of the deposited lithium could be controlled. with the delicate design of the microstructure and surface chemistry of Cu foam, such as microchannel construction[65,66] and ZnO[34,67] or graphene[68] decorations. In general, the 3D porous structure of Cu foam has shown greater advantages over 2D planar Cu foils in guiding lithium deposition.

Moreover, Cu-based alloy meshes are attractive starting materials for the preparation of functional porous lithiophilic architectures. Zhang *et al.* suggested a simple air annealing strategy to generate a homogenous ZnO coating layer on a commercial brass (CuZn alloy) mesh to realize highly stable lithium metal batteries operation.[64] The *in situ* formation of a lithiophilic ZnO layer on a commercial 3D brass mesh (ZnO–CuZn) by a facile air treatment at 300 °C is shown in Fig. 5c, based on the chemical energy release driven surface atom diffusion strategy. The voltage profiles demonstrated that the nucleation overpotential for the ZnO–CuZn mesh was as low as 65 mV, whereas that for the fresh CuZn mesh was 180 mV, indicating that the ZnO layer succeeded in reducing the nucleation overpotentials (Fig. 5d). Fig. 5e shows that the CE of ZnO–CuZn was maintained at 97.48% after 100 cycles, which was higher than that of the CuZn mesh (75%). Moreover, the voltage curves of the symmetrical cells with ZnO–CuZn mesh CCs delivered a prolonged lifespan of up to 1200 h with small polarization (Fig. 5f). The outstanding electrochemical performance could be attributed to the uniform lithiophilic ZnO coating and the 3D structure.

Similarly, Kang designed a 3D Cu nanowire-phosphide (CuNW-P) CC with a phosphidation gradient using a simple wet chemical method.[69] Beside the merits of 3D interconnected Cu nanowires, the phosphide gradient contributes to a high electrical and ionic conductivity, ensuring reversible Li deposition. Kim *et al.* compared the different behaviors of Li deposition/stripping in various CC structures. They concluded that the increased structural dimensions and hierarchy of CCs stabilized dendrite formation for extending the cycle life.

In this section, we introduced Cu-based current collectors, including surface modifications on Cu foil and designs of 3D porous Cu skeletons. Cu foil exists as the representative CC for commercial LIBs, which makes it an attractive starting material with high practicality and easy manufacturing. Nevertheless, a scalable approach must be developed to tune the lithiophobic nature of planar Cu foil to be lithiophilic before application in LMBs, which still requires further research. The implementation of 3D porous Cu skeleton obviously improves the electrochemical performance of LMAs, but the high material cost and low scalability make it unacceptable for commercialization. The currently reported Cu-based CCs show progress but still do not meet the high requirements of LMAs. Thus, approaches for novel cost-effective Cu-based current collectors with better performance are still worth exploring.

3. Beyond Cu foil

Modifications of Cu foils have been confirmed to be an effective strategy for improving the quality of the deposited lithium. The aforementioned 3D Cu CCs show great potential to further improve the electrochemical performance of LMBs. Therefore, it is worthwhile to develop more effective 3D porous Cu-based CCs, which would accelerate the exploration of LMBs. Meanwhile, more metallic and non-metallic materials should be considered when developing advanced CCs.

Compared with the Cu foil, the manufacturing cost of the Ni foil is relatively low, and Ni is more abundant than Cu in the Earth's crust. In addition, the electrochemical stability and mechanical strength of Ni are excellent. Ni foil is widely employed as a current collector in rechargeable batteries. However, Ni foil has a lithiophobic feature, which limits its practical application as a current collector for LMBs. Chen grew hexagonal plate lithiophilic NiO sheets on Ni foil (NiO-Ni) using a facile hydrothermal and thermal treatment method to guide uniform lithium deposition, as displayed in Fig. 6a.[70] NiO sheets worked to reduce nucleation barriers as Li^+ tended to react with NiO to form Ni/Li_2O first during the initial plating. The assembled 3D surface structure offers sufficient free space for lithium planting. The Li nucleation overpotentials of Ni and NiO-Ni were 33 and 17 mV, respectively, suggesting that polarization could be decreased by NiO seeds. The surface morphologies of Li-plated Ni and NiO-Ni further confirmed the role of the hexagonal plate NiO seeds, as shown in Fig. 6b and c.

Ni foam (NF) is more cost-effective than commercial Ni foil, and its 3D porous structure makes it more advantageous for inducing Li deposition. Li *et al.* constructed a nanoporous Ni foam (NPNF) CC through an atmosphere-controlled oxidation and reduction method.[71] Fig. 6d presents the distinct Li deposition process on pure Ni foam and nanoporous Ni foam CCs. The deposited Li tended to exhibit a dendrite-like morphology on the bare Ni foam. The nanoporous Ni foam possesses a larger surface area and evenly spaced nanopores, which can efficiently lower the local current density and guide uniform lithium nucleation and deposition with uniform Li^+ flux. As displayed in Fig. 6e, when the lithium-plated CCs were paired with a LFP cathode, the Li@NPNF‖LFP full cell exhibited an outstanding capacity retention of 93% after 300 cycles at a 1 C current density, along with a high CE of 99.5%, which was evidently better than that of the Li@NF‖LFP cell.

In addition to the aforementioned structural optimization, surface chemical modification is another common approach. By attaching an interconnected NiF_x nanosheets onto Ni foam (NiF_x@NF), the lithiophilicity of the framework can be greatly

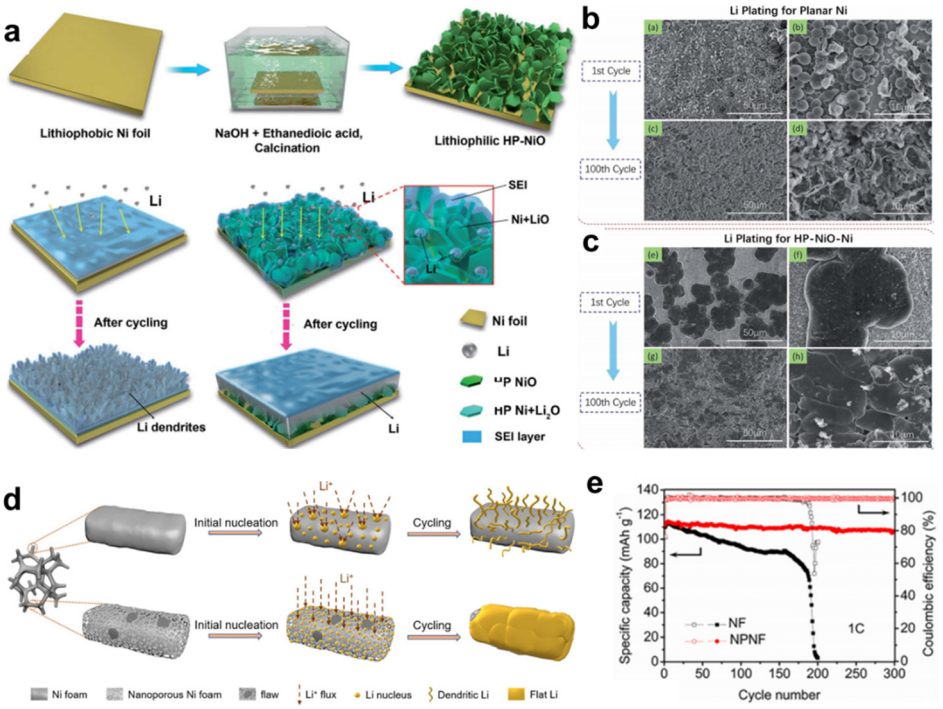

Fig. 6 Other metallic CCs. (a) Illustration of the growth of hexagonal plate lithiophilic NiO sheets on the Ni foil and corresponding lithium plating process. SEM images of the morphologies of Li plated onto (b) bare Ni substrate and (c) HP-NiO-Ni substrate. Reproduced with permission.[70] Copyright 2019 The Royal Society of Chemistry. (d) Schematics of Li deposition behavior on pure Ni foam and nanoporous Ni foam CCs. (e) Cycling performances of full cells of Li@NF‖LFP and Li@NPNF‖LFP. Reproduced with permission.[71] Copyright 2020 Elsevier B.V.

improved.[47] This fluorination process of Ni can be accomplished by a one-step thermal treatment with polytetrafluoroethylene powders as the fluorine precursor. A LiF-enriched SEI layer can be generated *in situ* during cycling to facilitate smooth Li growth. Ni_3S_2 nanosheets,[72] Co_3O_4 nanoarrays,[73] and $AuLi_3$ particles[48] have also been proven to be fine nucleation seeds to decorate Ni foam, which suppressed Li-dendrite growth and formed a stable SEI. Copper and nickel substrates are mostly used as metallic CCs. In addition, 3D stainless steel mesh and porous Ti foil have been proposed as typical metallic CCs.[74,75]

Research on metallic CCs is still proceeding rapidly; however, no desired results have been achieved. To achieve practical standards, efforts are being made to develop common metallic CCs. Simultaneously, measurable progress has been achieved in exploiting non-metal-based CCs.[76–78] Graphitic carbon-based CCs are the most representative non-metal collectors owing to their high conductivity and flexibility.[78]

Graphite materials are primarily used as nucleation sites or protection layers to modify metallic CCs, such as vertically aligned graphene pillars on Cu foil,[79] porous carbon nanotube (CNT) sponge on Cu foil,[43] fluorinated electrochemically exfoliated graphene coated on Cu foil,[80] and graphene anchored on Cu foam.[68] The mentioned graphene or CNT has an intrinsic nanostructure; accordingly, they can be easily attached to conductive substrates rather than fabricated into free-standing membranes. Recently, carbon fiber cloth emerged as an ideal choice for designing advanced CCs.[78] Carbon cloth has an inherent 3D structure, excellent flexibility, brilliant electrical conductivity, and free-standing characteristics. Liu *et al.* optimized commercial carbon cloth by graphene nesting and surface decoration for high-capacity lithium metal batteries.[81] A commercial carbon cloth was immersed in GO suspensions and zinc acetate solution stage by stage following by freeze-drying and annealing to prepare the final CFC/G/ZnO foil. Fig. 7a illustrates the morphology of the CFC/G/ZnO foil, where it can be observed that the graphene sheets located in the micro-channels of CF and ZnO nanoparticles decorated both on carbon fibers and graphene sheets. In addition, the possible mechanism of Li nucleation and growth on graphene sheets and carbon fibers was proposed. Li nucleated at ZnO sites and grew along the fibers or sheets. During the initial discharge, Li ions first intercalated into carbon materials and then started to nucleate and deposit, as shown in Fig. 7b. The CFC/G/ZnO presented a small overpotential of 4 mV at nucleation stage, which was much lower than that of Cu foil (29 mV). Modifying carbon cloth with lithiophilic materials like $Li_{22}Sn_5$ and Co nanoparticles to reduce nucleation barrier have also been proposed in other works.[82,83] Similarly, commercial graphite paper emerged as an available conductive matrix to design CCs as well.[84] To further improve the conductivity of the carbon framework, highly conductive copper layer cladding is a rational design.[85] By means of the 3D structure of the carbon framework, decorating on one side can elaborately guide the uniform Li deposition and avoid the impalement of separator by Li dendrites.[25]

Similar carbon framework can also be achieved by carbonization of paper[25] and growth on Ni foam substrate.[46,86] In a very

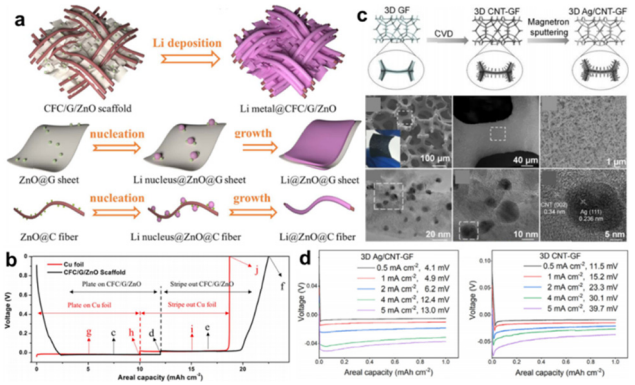

Fig. 7 Carbon based CCs. (a) Illustration of the structure of ZnO decorated carbon fiber cloth/graphene CC before and after plating of Li and the possible mechanism. (b) The stripping/plating profiles of Cu foil and CFC/G/ZnO CC paired with Li foil for half-cell test. Reproduced with permission.[81] Copyright 2018 Elsevier B.V. (c) Schematic diagram and morphology characterizations of the fabrication process of 3D Ag/CNT-GF nanostructures. (d) Overpotentials on 3D Ag/CNT-GF and 3D CNT-GF electrode. Reproduced with permission.[46] Copyright 2022 Elsevier B.V.

recent research proposed by Wang *et al.*, Ni foam was employed as a scaffold to prepare graphene foam by a general CVD method.[46] Carbon atoms deposited on Ni foam skeleton at 1000 °C under Ar/H_2 atmosphere, and graphene foam (GF) was formed after etching Ni by HCl solution. Moreover, CNTs were decorated onto the GF framework (3D CNT-GF) using the CVD method with NiCo catalysis. After Ag was sputtered onto the aforementioned structure, the final 3D Ag/CNT-GF substrate was obtained and used as a CC. Fig. 7c shows the fabrication process and morphology of the as-formed 3D Ag/CNT-GF. The 3D CNT-GF exhibited small nucleation overpotentials at current densities of 0.5–5 mA cm^{-2} (Fig. 7d). With additional Ag decoration, the overpotentials were further reduced, suggesting fast electrochemical kinetics on the 3D Ag/CNT-GF CCs. The excellent electrochemical performance is attributed to the high conductivity and surface area of the CNT-GF skeleton and the enhanced lithiophilicity of Ag.

Pre-storing lithium metal in a graphitic substrate instead of electrochemical deposition is a common strategy. Zhu *et al.* employed Ni foam as a template to adsorb graphene oxide (GO) dispersion, and reduced graphene oxide (rGO) foam was obtained by etching Ni and annealing.[87] Li metal was infused into rGO foam by directly contacting molten Li with rGO foam to form a Li/rGO composite. This rapid preparation process is called the spark reaction.[88] The rGO foam provides a flexible 3D structure that can efficiently alleviate the volume variation during Li plating and stripping. The Li/rGO composite could be directly paired with the NCM cathode to assemble a full cell without cumbersome prelithiation. Inspired by the spark reaction, carbon nanotubes have also been used as highly effective host materials to pre-store lithium, which has been found in recent studies.[44,89]

Compared to metallic materials, carbon materials can be tailored to the desired morphologies as the starting materials can be nanostructured GO, CNF, CNT, and various degradable organic carbon sources. The flexibility of carbon materials makes them favorable for assembly in flexible batteries, such as pouch cells.

Various carbon materials can be employed to design 3D porous CCs through both top-down and bottom-up methods, *e.g.*, chemical vapor deposition (from organic carbon source to graphene) and chemical exfoliation (from graphite to graphene), *etc.* The nano-micro- structure and chemical characteristics of carbon-based CCs can be well controlled, which can achieve enhanced electrochemical performance of LMAs as compared to Cu-based CCs. Nevertheless, none of the reported carbon-based CCs have the preparation methods and incompatibility with current manufacturing techniques.

4. Functional designs

Here, we introduce the advancements in CCs classified as per the categories of materials. Most of these CCs have been reported to enable Li nucleation and deposition, but they have rarely been confirmed to help form a stable SEI. Moreover, more attention should be paid to the safety hazards triggered by thermal runaway. Realizing dendrite-free Li plating/stripping is the first basic requisite for the operation of LMBs. Stabilizing the SEI layer is a critical factor in prolonging the lifespan of a single cell. Based on this, only improving the safety performance of LMBs can make them acceptable to industry and consumers. Herein, some functional designs for CCs are introduced.

SEI, that can be divided into *in situ* SEI and artificial SEI, significantly determines the battery performance.[90] The *in situ* SEI on CCs or deposited lithium is generated through a spontaneous electrochemical process, consisting of inner inorganic lithium compounds and outer organic components, which are fragile and highly reactive to the electrolyte during further cycling.[91–93] Artificial SEI are constructed on LMAs or CCs before cycling to induce smooth lithium deposition and alleviate parasitic reactions. Basically, artificial SEI must be electron insulated and ion conductive, and it should be homogenous in thickness and chemical composition and robust enough to accommodate the infinite volume change. Through, *ex situ* techniques, we can adopt highly ion-conductive and electrochemically stable inorganic components like LiF, Li_2S and Li_3N as artificial SEI and exclude inorganic materials like $ROCO_2Li$ or ROLi to avoid/mionimize side reactions.

The aforementioned lithiophilic particle decorations on the CCs mainly guided smooth Li deposition, which may not facilitate the prevention of continuous side reactions between freshly plated Li and the electrolyte and may generate a robust SEI layer. Deng *et al.* reported a super-ion-conductive lithium-rich antiperovskites film (LiRAP-ASEI) as an artificial SEI with a unique self-regulating phenomenon.[94] A molten state LiRAP was *in situ* produced and concurrently coated on the surface of Cu foil to form LiRAP-ASEI@Cu CC with the coating rod to control the thickness. Under the protection of the LiRAP-ASEI, the asymmetry cell delivered excellent stability with an

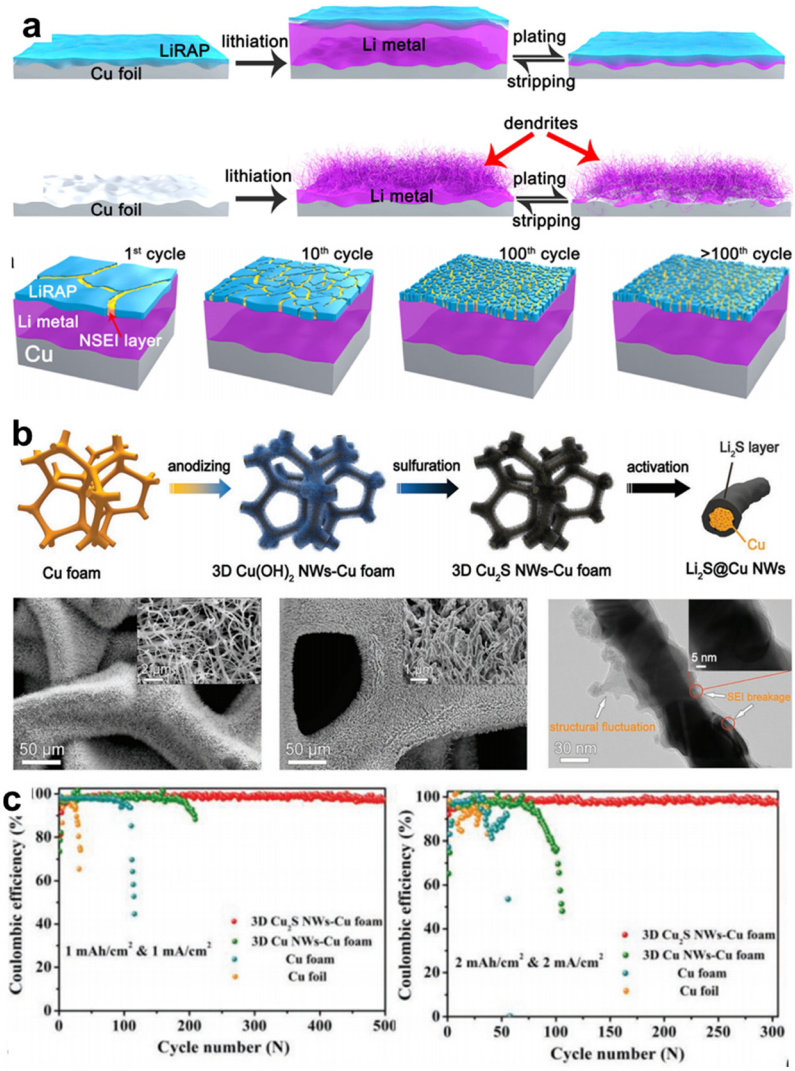

Fig. 8 SEI regulation by CCs. (a) Schematic illustration of the morphology changes of the lithium deposited on the copper foil substrate with (top) and without (middle) lithium-rich antiperovskites film, and the production process of the self-regulated LiRAP SEI layer after long cycling in the LiRAP/LiM/Cu alloy anode (down). Reproduced with permission.[94] Copyright 2020 American Chemical Society. (b) Fabrication and characterizations of the 3D Cu_2S NWs-Cu foam CC. (c) Coulombic efficiency of 3D Cu_2S NWs–Cu foam, 3D Cu NWs-Cu foam, Cu foam, and Cu foil. Reproduced with permission.[95] Copyright 2020 Wiley-VCH Verlag GmbH & Co. KGaA, Weinheim.

ultrahigh CE of 99.5% over 1500 cycles at 0.5 mA cm^{-2} and 0.5 mAh cm^{-2}. The Li plating/stripping behavior of bare Cu and LiRAP-ASEI@Cu and the possible self-regulating function of LiRAP-ASEI are shown in Fig. 8a. LiRAP-ASEI is expected to undergo repeated cracking and self-repair under the stress generated during Li deposition; thus, the SEI was able to dynamically maintain a mechanically robust protective layer.

Conformal polymer coatings on Cu foil have been reported to be effective protection layers, which facilitate the modification of the toughness of the SEI. Low-cost polyvinyl alcohol polymers,[42] high-polarity β-phase poly(vinylidene difluoride),[40] and PAN[96] have been confirmed to be promising artificial SEIs. In these studies, Li metal was preferentially deposited between Cu and the coating layer to reduce electrolyte consumption. Through the protection mechanism, the as-prepared full cells were able to operate in normal carbonate-based electrolytes.

Some inorganic materials have been determined to be effective at enhancing the strength and conductivity of SEI; for example, Li_3N,[36] LiF,[97] Li_3P,[63] and Li_2S.[95] Gong *et al.* employed Li_2S as an artificial SEI coating of Cu nanowires by *in situ* growth. Fig. 8b shows the synthesis process and morphology of the as-formed Li_2S@Cu NWs. Cu_2S NWs were grown on Cu foams by anodization (chronopotentiometry) and sulfuration. The surface Cu_2S was transferred to Li_2S during the initial activation process. The Li_2S artificial SEI exhibited an excellent structural stability and compositional homogeneity. Moreover, the high ionic conductivity of Li_2S can improve the electrode kinetics during the electrochemical process. Consequently, the asymmetric cells delivered high average CE of 99.2% over 500 cycles and 98.5% over 300 cycles when tested at 1 mA cm^{-2} and 2 mA cm^{-2} for 1h, as shown in Fig. 8c. The enhanced CEs are attributed to the strong

mechanical and electrochemical stability of the artificial Li_2S SEI layer.

With a stable SEI, LMBs provide an enhanced service time, which can be directly represented by the cycles of full cells. However, the thermal runaway issues should be tackled before putting the cell into the market. In general, thermal runaway can be caused by mechanical, electrical, and thermal abuse, accompanied by smoke, fire and explosion.[98] In the literature on thermal runaway issues in LMBs, researchers have mainly worked on separator modifications and electrolyte optimizations to decrease the risks, while few reports have focused on the role of CCs. Here, we refer to the brilliant work on fire-extinguishing CCs for high-energy LIBs proposed by Cui *et al.*[99] They reported an ultralight polyimide-based CC prepared by sandwiching a polyimide (PI) and triphenyl phosphate (TPP) composite between two thin Cu layers (PI-TPP-Cu). Polyimides offer a lightweight skeleton and exhibit thermal retardant features. Triphenyl phosphate was selected as the flame-retardant material owing to its low melting point and low cost. Cu layers were used to collect electrons. Upon exposure to an open flame, the pouch cell based on PI-TPP-Cu burned infirmly and self-extinguished quickly within 6 s.

PI-TPP-Cu CCs have attracted significant interest and have been commercialized. However, similar CC designs for LMBs have not yet been reported. LMB faces more complicated and serious thermal runaway problems because of its high reactivity and uncontrollable Li growth. Therefore, the investigation and research on fire-extinguishing CCs in LMBs systems should be conducted. Numerous flame-extinguishing materials have been reported and applied in various fields, including phosphorus compounds,[100,101] mineral xonotlite $Ca_6Si_6O_{17}(OH)_2$,[102] and $Mg(OH)_2$,[103] among others. A better understanding of the flame-retardant characteristics and their application to integrated CCs could stimulate future development, which is highly encouraged.

In this section, we introduced some specially designed CCs that could further meet the high requirement of LMBs in addition to electrochemical performance. Since LMAs face more stringent safety issues due to dendrite growth and unstable SEI issues, it is believed that CCs could reduce safety concerns to some extent. The above-mentioned CCs have made great but not sufficient progress, and they were evaluated under limited conditions. Thus, future current collectors should be comprehensively characterized in terms of thie electrochemical stability, safety, cost and scale-up capability.

5. Conclusion and outlook

Lithium metal anodes operate *via* electrodeposition. Accordingly, lithiophobic Cu foils are not applicable in LMB systems. Modifying the Cu foil with lithiophilic materials is an effective strategy to reduce nucleation barriers and achieve dendrite-free Li deposition. The decorations on the Cu foil could be particles, 1D nanotubes and nanofibers, 2D films, and 3D conformal coatings. Dendrite-free deposition can be realized by delicately constructing 3D porous structures that allow lithium to preferentially deposit into the pores. Moreover, nickel- and carbon-based materials have been proposed as efficient substrates to enable smooth Li deposition. In addition, flame-retardant and wide-temperature operation should be the final target to realize the applications of lithium metal batteries.

In some studies, Li nucleated at the lithiophilic region and grew towards the separator. Under these circumstances, unevenly deposited Li metal may eventually impale the separator, and the exposed Li inevitably reacts with the electrolyte, leading to a low CE. It would be better to guide Li growth away from the separator with the aid of a functional coating layer on the CCs. The coating layer not only blocks direct contact between Li and the electrolyte but also facilitates Li^+ ion transportation, and the coating layer is called an artificial SEI. However, functional chemistry modification is expected to reduce adverse reactions by constructing a robust ion-conductive SEI. A combination of the two methods has not been reported, but it is worth exploring.

Numerous studies have reported dendrite-free Li plating. However, a coulombic efficiency of 94–99% has been considered as good in many studies. It was progressing compared to previous studies, but still far from practical applications. Broader concerns regarding the coulombic efficiency, SEI stability, and cyclability should be raised. In this regard, a comprehensive understanding on the evolution of deposited Li, SEI and the failure mechanism of lithium metal anodes will guide future research.

As the exploration of lithium metal anodes is still in progress, investigating the applications of some novel materials, such as graphene, graphdiyne, metal organic frameworks (MOFs), covalent organic frameworks, and MXene, for modifying CCs is worthwhile. For example, a lithiophilic metal atom can be plated in the MOF to deposit lithium into the porous structure of the MOF; thus, dendritic lithium will be avoided.

The crossover effect between Li anodes and cathodes was confirmed. Nevertheless, few reports have mentioned the crossover effect between anode CCs and cathodes. This is crucial for designing anode-free lithium ion batteries, as dissolved atoms from cathodes may travel to the anode side and impact the lithium deposition behavior. Thus, the best cathode that can be well-paired with a lithium metal anode or anode-free configuration can be determined.

Although solid state electrolytes hold great promise in (anode-free) lithium metal batteries, the interaction between current collectors and solid-state electrolytes remains unclear and the related CCs are insufficiently developed thus far. Most research investigated the feasibility of CCs in non-aqueous liquid electrolytes, which might not ultimately be the ideal system for LMBs when considering the merits of solid state electrolytes. Hence, the performance of the mentioned CCs and beyond should be further examined in solid state batteries.

Finally, we should upgrade the existing industrial techniques to develop lithium metal batteries, as high-tech industrial bases and chains for manufacturing lithium ion batteries are already present. In this way, lithium metal batteries will meet the required demand.

Conflicts of interest

The authors declare no conflict of interest.

Acknowledgements

MHR thanks the National Natural Science Foundation of China (Grant No. 52071225 and 51672181), Department of Human Resources and Social Security of Jiangsu Province (100 Talents Project), the Czech Republic from ERDF ''Institute of Environmental Technology-Excellent Research'' (No. CZ.02.1.01/0.0/0.0/16_019/0000853), and the SinoGerman Research Institute for their support (Project GZ 1400).

References

1 X. Xia, J. Luo, Z. Zeng, C. Guan, Y. Zhang, J. Tu, H. Zhang and H. J. Fan, Integrated photoelectrochemical energy storage: solar hydrogen generation and supercapacitor, *Sci. Rep.*, 2012, **2**, 981.

2 Y. Chen, Y. Luo, H. Zhang, C. Qu, H. Zhang and X. Li, The Challenge of Lithium Metal Anodes for Practical Applications, *Small Methods*, 2019, **3**, 1800551.

3 J. B. Goodenough, Evolution of Strategies for Modern Rechargeable Batteries, *Acc. Chem. Res.*, 2013, **46**, 1053–1061.

4 X.-Q. Xu, X.-B. Cheng, F.-N. Jiang, S.-J. Yang, D. Ren, P. Shi, H. Hsu, H. Yuan, J.-Q. Huang, M. Ouyang and Q. Zhang, Dendrite-accelerated thermal runaway mechanisms of lithium metal pouch batteries, *SusMat*, 2022, **2**, 435–444.

5 S.-J. Yang, N. Yao, F.-N. Jiang, J. Xie, S.-Y. Sun, X. Chen, H. Yuan, X.-B. Cheng, J.-Q. Huang and Q. Zhang, Thermally Stable Polymer-Rich Solid Electrolyte Interphase for Safe Lithium Metal Pouch Cells, *Angew. Chem., Int. Ed.*, 2022, **61**, e202214545.

6 R. Chen, A. M. Nolan, J. Lu, J. Wang, X. Yu, Y. Mo, L. Chen, X. Huang and H. Li, The Thermal Stability of Lithium Solid Electrolytes with Metallic Lithium, *Joule*, 2020, **4**, 812–821.

7 L. Huang, T. Lu, G. Xu, X. Zhang, Z. Jiang, Z. Zhang, Y. Wang, P. Han, G. Cui and L. Chen, Thermal runaway routes of large-format lithium-sulfur pouch cell batteries, *Joule*, 2022, **6**, 906–922.

8 F.-N. Jiang, S.-J. Yang, X.-B. Cheng, P. Shi, J.-F. Ding, X. Chen, H. Yuan, L. Liu, J.-Q. Huang and Q. Zhang, Thermal safety of dendritic lithium against non-aqueous electrolyte in pouch-type lithium metal batteries, *J. Energy Chem.*, 2022, **72**, 158–165.

9 J. Tu, W. Wang, H. Lei, M. Wang, C. Chang and S. Jiao, Design Strategies of High-Performance Positive Materials for Nonaqueous Rechargeable Aluminum Batteries: From Crystal Control to Battery Configuration, *Small*, 2022, **18**, 2201362.

10 M. Chen, M. Shao, J. Jin, L. Cui, H. Tu and X. Fu, Configurational and structural design of separators toward shuttling-free and dendrite-free lithium-sulfur batteries: A review, *Energy Storage Mater.*, 2022, **47**, 629–648.

11 S. Jin, Y. Jiang, H. Ji and Y. Yu, Advanced 3D Current Collectors for Lithium-Based Batteries, *Adv. Mater.*, 2018, **30**, 1802014.

12 D. Li, H. Hu, B. Chen and W.-Y. Lai, Advanced Current Collector Materials for High-Performance Lithium Metal Anodes, *Small*, 2022, **18**, 2200010.

13 Y. Liu, D. Gao, H. Xiang, X. Feng and Y. Yu, Research Progress on Copper-Based Current Collector for Lithium Metal Batteries, *Energy Fuels*, 2021, **35**, 12921–12937.

14 Y. Liu, Y. Li, J. Sun, Z. Du, X. Hu, J. Bi, C. Liu, W. Ai and Q. Yan, Present and future of functionalized Cu current collectors for stabilizing lithium metal anodes, *Nano Res. Energy*, 2023, **2**, e9120048.

15 X. Shen, H. Liu, X.-B. Cheng, C. Yan and J.-Q. Huang, Beyond lithium ion batteries: Higher energy density battery systems based on lithium metal anodes, *Energy Storage Mater.*, 2018, **12**, 161–175.

16 Z. Li, J. Huang, B. Y. Liaw, V. Metzler and J. Zhang, A review of lithium deposition in lithium-ion and lithium metal secondary batteries, *J. Power Sources*, 2014, **254**, 168–182.

17 A. Gabryelczyk, S. Ivanov, A. Bund and G. Lota, Corrosion of aluminium current collector in lithium-ion batteries: A review, *J. Energy Storage*, 2021, **43**, 103226.

18 B. Zhou, A. Bonakdarpour, I. Stosevski, B. Fang and D. P. Wilkinson, Modification of Cu current collectors for lithium metal batteries – A review, *Prog. Mater. Sci.*, 2022, **130**, 100996.

19 E. Cha, J. H. Yun, R. Ponraj and D. K. Kim, A mechanistic review of lithiophilic materials: resolving lithium dendrites and advancing lithium metal-based batteries, *Mater. Chem. Front.*, 2021, **5**, 6294–6314.

20 J. Chen, J. Xiang, X. Chen, L. Yuan, Z. Li and Y. Huang, Li_2S-based anode-free full batteries with modified Cu current collector, *Energy Storage Mater.*, 2020, **30**, 179–186.

21 G. Hou, Q. Sun, Q. Ai, X. Ren, X. Xu, H. Guo, S. Guo, L. Zhang, J. Feng, F. Ding, P. M. Ajayan, P. Si and L. Ci, Growth direction control of lithium dendrites in a heterogeneous lithiophilic host for ultra-safe lithium metal batteries, *J. Power Sources*, 2019, **416**, 141–147.

22 H. Zheng, Q. Zhang, Q. Chen, W. Xu, Q. Xie, Y. Cai, Y. Ma, Z. Qiao, Q. Luo, J. Lin, L. Wang, B. Qu, B. Sa and D.-L. Peng, 3D lithiophilic–lithiophobic–lithiophilic dualgradient porous skeleton for highly stable lithium metal anode, *J. Mater. Chem. A*, 2020, **8**, 313–322.

23 W.-B. Jung, O. B. Chae, M. Kim, Y. Kim, Y. J. Hong, J. Y. Kim, S. Choi, D. Y. Kim, S. Moon, J. Suk, Y. Kang, M. Wu and H.-T. Jung, Effect of Highly Periodic Au Nanopatterns on Dendrite Suppression in Lithium Metal Batteries, *ACS Appl. Mater. Interfaces*, 2021, **13**, 60978–60986.

24 J. Pu, J. Li, Z. Shen, C. Zhong, J. Liu, H. Ma, J. Zhu, H. Zhang and P. V. Braun, Interlayer Lithium Plating in Au Nanoparticles Pillared Reduced Graphene Oxide for Lithium Metal Anodes, *Adv. Funct. Mater.*, 2018, **28**, 1804133.

25 B. Hong, H. Fan, X.-B. Cheng, X. Yan, S. Hong, Q. Dong, C. Gao, Z. Zhang, Y. Lai and Q. Zhang, Spatially uniform

deposition of lithium metal in 3D Janus hosts, *Energy Storage Mater.*, 2019, **16**, 259–266.
26 W. Shin and A. Manthiram, Fast and Simple Ag/Cu Ion Exchange on Cu Foil for Anode-Free Lithium-Metal Batteries, *ACS Appl. Mater. Interfaces*, 2022, **14**, 17454–17460.
27 Z. T. Wondimkun, W. A. Tegegne, J. Shi-Kai, C.-J. Huang, N. A. Sahalie, M. A. Weret, J.-Y. Hsu, P.-L. Hsieh, Y.-S. Huang, S.-H. Wu, W.-N. Su and B. J. Hwang, Highly-lithiophilic Ag@PDA-GO film to Suppress Dendrite Formation on Cu Substrate in Anode-free Lithium Metal Batteries, *Energy Storage Mater.*, 2021, **35**, 334–344.
28 Z. Hou, Y. Yu, W. Wang, X. Zhao, Q. Di, Q. Chen, W. Chen, Y. Liu and Z. Quan, Lithiophilic Ag Nanoparticle Layer on Cu Current Collector toward Stable Li Metal Anode, *ACS Appl. Mater. Interfaces*, 2019, **11**, 8148–8154.
29 G. Wang, X. Xiong, P. Zou, X. Fu, Z. Lin, Y. Li, Y. Liu, C. Yang and M. Liu, Lithiated zinc oxide nanorod arrays on copper current collectors for robust Li metal anodes, *Chem. Eng. J.*, 2019, **378**, 122243.
30 C. Zhang, W. Lv, G. Zhou, Z. Huang, Y. Zhang, R. Lyu, H. Wu, Q. Yun, F. Kang and Q.-H. Yang, Vertically Aligned Lithiophilic CuO Nanosheets on a Cu Collector to Stabilize Lithium Deposition for Lithium Metal Batteries, *Adv. Energy Mater.*, 2018, **9**, 1703404.
31 Q. Zhang, J. Luan, Y. Tang, X. Ji, S. Wang and H. Wang, A facile annealing strategy for achieving in situ controllable Cu2O nanoparticle decorated copper foil as a current collector for stable lithium metal anodes, *J. Mater. Chem. A*, 2018, **6**, 18444–18448.
32 Z. Gong, C. Lian, P. Wang, K. Huang, K. Zhu, K. Ye, J. Yan, G. Wang and D. Cao, Lithiophilic Cu-Li_2O matrix on a Cu Collector to Stabilize Lithium Deposition for Lithium Metal Batteries, *Energy Environ. Mater.*, 2022, **5**, 1270–1277.
33 R. Guan, S. Liu, C. Wang, Y. Yang, D. Lu and X. Bian, Lithiophilic Sn sites on 3D Cu current collector induced uniform lithium plating/stripping, *Chem. Eng. J.*, 2021, **425**, 130177.
34 Y. Zhou, K. Zhao, Y. Han, Z. Sun, H. Zhang, L. Xu, Y. Ma and Y. Chen, A nitrogen-doped-carbon/ZnO modified Cu foam current collector for high-performance Li metal batteries, *J. Mater. Chem. A*, 2019, **7**, 5712–5718.
35 S. T. Oyakhire, W. Zhang, A. Shin, R. Xu, D. T. Boyle, Z. Yu, Y. Ye, Y. Yang, J. A. Raiford, W. Huang, J. R. Schneider and Y. Cui, Electrical resistance of the current collector controls lithium morphology, *Nat. Commun.*, 2022, **13**, 3986.
36 D. Tang, L. Yuan, Y. Liao, W. Jin, J. Chen, Z. Cheng, X. Li, B. He, Z. Li and Y. Huang, Improving the cycling stability of lithium metal anodes using Cu3N-modified Cu foil as a current collector, *Sci. China Mater.*, 2022, **65**, 2385–2392.
37 W. Chen, R. V. Salvatierra, M. Ren, J. Chen, M. G. Stanford and J. M. Tour, Laser-Induced Silicon Oxide for Anode-Free Lithium Metal Batteries, *Adv. Mater.*, 2020, **32**, 2002850.
38 J. Yi, J. Chen, Z. Yang, Y. Dai, W. Li, J. Cui, F. Ciucci, Z. Lu and C. Yang, Facile Patterning of Laser-Induced Graphene with Tailored Li Nucleation Kinetics for Stable Lithium-Metal Batteries, *Adv. Energy Mater.*, 2019, **9**, 1901796.
39 Y. He, H. Xu, J. Shi, P. Liu, Z. Tian, N. Dong, K. Luo, X. Zhou and Z. Liu, Polydopamine Coating Layer Modified Current Collector for Dendrite-Free Li Metal Anode, *Energy Storage Mater.*, 2019, **23**, 418–426.
40 J. Luo, C.-C. Fang and N.-L. Wu, High Polarity Poly(vinylidene difluoride) Thin Coating for Dendrite-Free and High-Performance Lithium Metal Anodes, *Adv. Energy Mater.*, 2018, **8**, 1701482.
41 A. A. Assegie, J.-H. Cheng, L.-M. Kuo, W.-N. Su and B.-J. Hwang, Polyethylene oxide film coating enhances lithium cycling efficiency of an anode-free lithium-metal battery, *Nanoscale*, 2018, **10**, 6125–6138.
42 Y. Zhao, D. Wang, Y. Gao, T. Chen, Q. Huang and D. Wang, Stable Li metal anode by a polyvinyl alcohol protection layer via modifying solid-electrolyte interphase layer, *Nano Energy*, 2019, **64**, 103893.
43 F. Shen, F. Zhang, Y. Zheng, Z. Fan, Z. Li, Z. Sun, Y. Xuan, B. Zhao, Z. Lin, X. Gui, X. Han, Y. Cheng and C. Niu, Direct growth of 3D host on Cu foil for stable lithium metal anode, *Energy Storage Mater.*, 2018, **13**, 323–328.
44 Z. Wang, Z. Lu, W. Guo, Q. Luo, Y. Yin, X. Liu, Y. Li, B. Xia and Z. Wu, A Dendrite-Free Lithium/Carbon Nanotube Hybrid for Lithium-Metal Batteries, *Adv. Mater.*, 2021, **33**, 2006702.
45 L. K. Ventrapragada, S. E. Creager, A. M. Rao and R. Podila, Carbon Nanotubes Coated Paper as Current Collectors for Secondary Li-ion Batteries, *Nanotechnol. Rev.*, 2019, **8**, 18–23.
46 B. Tian, Z. Huang, X. Xu, X. Cao, H. Wang, T. Xu, D. Kong, Z. Zhang, J. Xu, J. Zang, X. Li and Y. Wang, Three-dimensional Ag/carbon nanotube-graphene foam for high performance dendrite free lithium/sodium metal anodes, *J. Mater. Sci. Technol.*, 2023, **132**, 50–58.
47 G. Huang, S. Chen, P. Guo, R. Tao, K. Jie, B. Liu, X. Zhang, J. Liang and Y.-C. Cao, In situ constructing lithiophilic NiF_x nanosheets on Ni foam current collector for stable lithium metal anode via a succinct fluorination strategy, *Chem. Eng. J.*, 2020, **395**, 125122.
48 X. Ke, Y. Liang, L. Ou, H. Liu, Y. Chen, W. Wu, Y. Cheng, Z. Guo, Y. Lai, P. Liu and Z. Shi, Surface engineering of commercial Ni foams for stable Li metal anodes, *Energy Storage Mater.*, 2019, **23**, 547–555.
49 Y. Shi, Z. Wang, H. Gao, J. Niu, W. Ma, J. Qin, Z. Peng and Z. Zhang, A self-supported, three-dimensional porous copper film as a current collector for advanced lithium metal batteries, *J. Mater. Chem. A*, 2019, **7**, 1092–1098.
50 D. Zhang, A. Dai, M. Wu, K. Shen, T. Xiao, G. Hou, J. Lu and Y. Tang, Lithiophilic 3D Porous CuZn Current Collector for Stable Lithium Metal Batteries, *ACS Energy Lett.*, 2020, **5**, 180–186.
51 Y. An, H. Fei, G. Zeng, X. Xu, L. Ci, B. Xi, S. Xiong, J. Feng and Y. Qian, Vacuum distillation derived 3D porous current collector for stable lithium–metal batteries, *Nano Energy*, 2018, **47**, 503–511.
52 H. Liu, E. Wang, Q. Zhang, Y. Ren, X. Guo, L. Wang, G. Li and H. Yu, Unique 3D nanoporous/macroporous structure

Cu current collector for dendrite-free lithium deposition, *Energy Storage Mater.*, 2019, **17**, 253–259.
53 R. Zhang, S. Wen, N. Wang, K. Qin, E. Liu, C. Shi and N. Zhao, N-Doped Graphene Modified 3D Porous Cu Current Collector toward Microscale Homogeneous Li Deposition for Li Metal Anodes, *Adv. Energy Mater.*, 2018, **8**, 1800914.
54 X. F. Tan, S. D. McDonald, Q. Gu, Y. Hu, L. Wang, S. Matsumura, T. Nishimura and K. Nogita, Characterisation of lithium-ion battery anodes fabricated *via in situ* Cu6Sn5 growth on a copper current collector, *J. Power Sources*, 2019, **415**, 50–61.
55 D. Liu, Y. Wang, T. Tong, G. Luo, J. Shen and X. Cai, Mesoporous copper-based metal glass as current collector for Li metal anode, *Chem. Eng. J.*, 2023, **451**, 138910.
56 J. Chen, J. Zhao, L. Lei, P. Li, J. Chen, Y. Zhang, Y. Wang, Y. Ma and D. Wang, Dynamic Intelligent Cu Current Collectors for Ultrastable Lithium Metal Anodes, *Nano Lett.*, 2020, **20**, 3403–3410.
57 Y. Tang, K. Shen, Z. Lv, X. Xu, G. Hou, H. Cao, L. Wu, G. Zheng and Y. Deng, Three-dimensional ordered macroporous Cu current collector for lithium metal anode: Uniform nucleation by seed crystal, *J. Power Sources*, 2018, **403**, 82–89.
58 S. M. Jeong, M. Wu, T. Y. Kim, D. H. Kim, S.-H. Kim, H. K. Choi, Y. C. Kang and D. Y. Kim, A 3D Porous Inverse Opal Ni Structure on a Cu Current Collector for Stable Lithium-Metal Batteries, *Batteries Supercaps*, 2022, **5**, e202100257.
59 Y. Xie, H. Zhang, J. Yu, Z. Liu, S. Zhang, H. Shao, Y. Cao, X. Huang and S. Li, A Novel Dendrite-Free Lithium Metal Anode *via* Oxygen and Boron Codoped Honeycomb Carbon Skeleton, *Small*, 2022, **18**, 2104876.
60 X. Cao, Q. Wang, H. Wang, Z. Shang, J. Qin, W. Liu, H. Zhou and X. Sun, *Mater. Chem. Front.*, 2021, **5**, 5486.
61 H. Qiu, T. Tang, M. Asif, X. Huang and Y. Hou, 3D Porous Cu Current Collectors Derived by Hydrogen Bubble Dynamic Template for Enhanced Li Metal Anode Performance, *Adv. Funct. Mater.*, 2019, **29**, 1808468.
62 Y. Chen, A. Elangovan, D. Zeng, Y. Zhang, H. Ke, J. Li, Y. Sun and H. Cheng, Vertically Aligned Carbon Nanofibers on Cu Foil as a 3D Current Collector for Reversible Li Plating/Stripping toward High-Performance Li–S Batteries, *Adv. Funct. Mater.*, 2020, **30**, 1906444.
63 Y. Zhao, S. Hao, L. Su, Z. Ma and G. Shao, Hierarchical Cu fibers induced Li uniform nucleation for dendrite-free lithium metal anode, *Chem. Eng. J.*, 2020, **392**, 123691.
64 S. Huang, W. Zhang, H. Ming, G. Cao, L.-Z. Fan and H. Zhang, Chemical Energy Release Driven Lithiophilic Layer on 1 m^2 Commercial Brass Mesh toward Highly Stable Lithium Metal Batteries, *Nano Lett.*, 2019, **19**, 1832–1837.
65 J. Wang, M. Wang, F. Chen, Y. Li, L. Zhang, Y. Zhao and C. Chen, In-situ construction of lithiophilic interphase in vertical micro-channels of 3D copper current collector for high performance lithium-metal batteries, *Energy Storage Mater.*, 2021, **34**, 22–27.
66 F. Pei, A. Fu, W. Ye, J. Peng, X. Fang, M.-S. Wang and N. Zheng, Robust Lithium Metal Anodes Realized by Lithiophilic 3D Porous Current Collectors for Constructing High-Energy Lithium−Sulfur Batteries, *ACS Nano*, 2019, **13**, 8337–8346.
67 J. Zhang, H. Chen, M. Wen, K. Shen, Q. Chen, G. Hou and Y. Tang, Lithiophilic 3D Copper-Based Magnetic Current Collector for Lithium-Free Anode to Realize Deep Lithium Deposition, *Adv. Funct. Mater.*, 2022, **32**, 2110110.
68 G. Yang, J. Chen, P. Xiao, P. O. Agboola, I. Shakir and Y. Xu, Graphene anchored on Cu foam as a lithiophilic 3D current collector for a stable and dendrite-free lithium metal anode, *J. Mater. Chem. A*, 2018, **6**, 9899–9905.
69 C. Zhang, R. Lyu, W. Lv, H. Li, W. Jiang, J. Li, S. Gu, G. Zhou, Z. Huang, Y. Zhang, J. Wu, Q.-H. Yang and F. Kang, A Lightweight 3D Cu Nanowire Network with Phosphidation Gradient as Current Collector for High-Density Nucleation and Stable Deposition of Lithium, *Adv. Mater.*, 2019, **31**, 1904991.
70 W. Lu, C. Wu, W. Wei, J. Ma, L. Chen and Y. Chen, Lithiophilic NiO hexagonal plates decorated Ni collector guiding uniform lithium plating for stable lithium metal anode, *J. Mater. Chem. A*, 2019, **7**, 24262–24270.
71 S. Liu, H. Zhang, X. Liu, Y. Yang, C. Chi, S. Wang, J. Xue, T. Hao, J. Zhao and Y. Li, Constructing nanoporous Ni foam current collectors for stable lithium metal anodes, *J. Energy Chem.*, 2021, **58**, 124–132.
72 J. Zhang, Y. Zhou, F. Tu, Y. Ma, H. Zhang, D. Song, X. Shi and L. Zhang, In situ constructing lithiophilic and Ion/Electron Dual-Regulated current collector for highly stable lithium metal batteries, *Chem. Eng. J.*, 2022, **428**, 132510.
73 C. Guo, Y. Guo, R. Tao, X. Liao, K. Du, H. Zou, W. Zhang, J. Liang, D. Wang, X. Sun and S. Lu, Uniform lithiophilic layers in 3D current collectors enable ultrastable solid electrolyte interphase for high-performance lithium metal batteries, *Nano Energy*, 2022, **96**, 107121.
74 X. Zhang, A. Wang, R. Lv and J. Luo, A corrosion-resistant current collector for lithium metal anodes, *Energy Storage Mater.*, 2019, **18**, 199–204.
75 H. Kim, Y. J. Gong, J. Yoo and Y. S. Kim, Highly stable lithium metal battery with an applied three-dimensional mesh structure interlayer, *J. Mater. Chem. A*, 2018, **6**, 15540–15545.
76 P. Zhu, D. Gastol, J. Marshall, R. Sommerville, V. Goodship and E. Kendrick, A review of current collectors for lithium-ion batteries, *J. Power Sources*, 2021, **485**, 229321.
77 L. Hu, J. Deng, Q. Liang, J. Wu, B. Ge, Q. Liu, G. Chen and X. Yu, Engineering current collectors for advanced alkali metal anodes: A review and perspective, *EcoMat*, 2022, e12269.
78 S. Zhang, S. Xiao, D. Li, J. Liao, F. Ji, H. Liu and L. Ci, Commercial carbon cloth: An emerging substrate for practical lithium metal batteries, *Energy Storage Mater.*, 2022, **48**, 172–190.
79 K. Lin, X. Xu, X. Qin, S. Wang, C. Han, H. Geng, X. Li, F. Kang, G. Chen and B. Li, Dendrite-free lithium

deposition enabled by a vertically aligned graphene pillar architecture, *Carbon*, 2021, **185**, 152–160.

80 A. Jamaluddin, Y.-Y. Sin, E. Adhitama, A. Prayogi, Y.-T. Wu, J.-K. Chang and C.-Y. Su, Fluorinated graphene as a dual-functional anode to achieve dendrite-free and high-performance lithium metal batteries, *Carbon*, 2022, **197**, 141–151.

81 W. Deng, W. Zhu, X. Zhou and Z. Liu, Graphene nested porous carbon current collector for lithium metal anode with ultrahigh areal capacity, *Energy Storage Mater.*, 2018, **15**, 266–273.

82 Y. Liu, Z. Song, Z. Wang, J. Xing, W. Zou and J. Li, Regulating Li nucleation/deposition by bamboo-shoot like lithiophilic particles anchored on carbon cloth for a dendrite-free lithium metal anode, *Mater. Chem. Front.*, 2023, **7**, 117–127.

83 C. Lu, Z. Gao, B. Liu, Z. Shi, Y. Yi, W. Zhao, W. Guo, Z. Liu and J. Sun, Synchronous Promotion in Sodiophilicity and Conductivity of Flexible Host via Vertical Graphene Cultivator for Longevous Sodium Metal Batteries, *Adv. Funct. Mater.*, 2021, **31**, 2101233.

84 Z. Huang, D. Kong, Y. Zhang, Y. Deng, G. Zhou, C. Zhang, F. Kang, W. Lv and Q.-H. Yang, Vertical Graphenes Grown on a Flexible Graphite Paper as an All-Carbon Current Collector towards Stable Li Deposition, *Research*, 2020, **2020**, 7163948.

85 K. Chen, R. Pathak, A. Gurung, K. M. Reza, N. Ghimire, J. Pokharel, A. Baniya, W. He, J. J. Wu, Q. Qiao and Y. Zhou, A copper-clad lithiophilic current collector for dendrite-free lithium metal anodes, *J. Mater. Chem. A*, 2020, **8**, 1911–1919.

86 F. Liu, S. Chiluwal, A. S. Childress, C. Etteh, K. Miller, M. Washington, A. M. Rao and R. Podila, Graphene Foam Current Collector for High-Areal-Capacity Lithium− Sulfur Batteries, *ACS Appl. Nano Mater.*, 2021, **4**, 53–60.

87 P. Yao, Q. Chen, Y. Mu, J. Liang, X. Li, X. Liu, Y. Wang, B. Zhu and J. Zhu, 3D hollow reduced graphene oxide foam as a stable host for high-capacity lithium metal anodes, *Mater. Chem. Front.*, 2019, **3**, 339–343.

88 D. Lin, Y. Liu, Z. Liang, H.-W. Lee, J. Sun, H. Wang, K. Yan, J. Xie and Y. Cui, Layered reduced graphene oxide with nanoscale interlayer gaps as a stable host for lithium metal anodes, *Nat. Nanotechnol.*, 2016, **11**, 626–632.

89 J. Wang, H. Liu, H. Wu, Q. Li, Y. Zhang, S. Fan and J. Wang, Self-standing carbon nanotube aerogels with amorphous carbon coating as stable host for lithium anodes, *Carbon*, 2021, **177**, 181–188.

90 X. Shan, Y. Zhong, L. Zhang, Y. Zhang, X. Xia, X. Wang and J. Tu, A Brief Review on Solid Electrolyte Interphase Composition Characterization Technology for Lithium Metal Batteries: Challenges and Perspectives, *J. Phys. Chem. C*, 2021, **125**, 19060–19080.

91 Y. Jie, X. Ren, R. Cao, W. Cai and S. Jiao, Advanced Liquid Electrolytes for Rechargeable Li Metal Batteries, *Adv. Funct. Mater.*, 2020, **30**, 1910777.

92 K. Qin, K. Holguin, M. Mohammadiroudbari, J. Huang, E. Y. S. Kim, R. Hall and C. Luo, Strategies in Structure and Electrolyte Design for High-Performance Lithium Metal Batteries, *Adv. Funct. Mater.*, 2021, **31**, 2009694.

93 J.-G. Zhang, W. Xu, J. Xiao, X. Cao and J. Liu, Lithium Metal Anodes with Nonaqueous Electrolytes, *Chem. Rev.*, 2020, **120**, 13312–13348.

94 B. Han, D. Feng, S. Li, Z. Zhang, Y. Zou, M. Gu, H. Meng, C. Wang, K. Xu, Y. Zhao, H. Zeng, C. Wang and Y. Deng, Self-Regulated Phenomenon of Inorganic Artificial Solid Electrolyte Interphase for Lithium Metal Batteries, *Nano Lett.*, 2020, **20**, 4029–4037.

95 P. Zhai, Y. Wei, J. Xiao, W. Liu, J. Zuo, X. Gu, W. Yang, S. Cui, B. Li, S. Yang and Y. Gong, In Situ Generation of Artificial Solid-Electrolyte Interphases on 3D Conducting Scaffolds for High-Performance Lithium-Metal Anodes, *Adv. Energy Mater.*, 2020, **10**, 1903339.

96 Y. Liu, Y. Xu, J. Wang, Y. Sun, X. Feng and H. Xiang, Regulated lithium deposition behavior by an artificial coating of Cu foil for dendrite-free lithium metal batteries, *Mater. Today Sustain.*, 2022, **18**, 100127.

97 X. Fan, X. Ji, F. Han, J. Yue, J. Chen, L. Chen, T. Deng, J. Jiang and C. Wang, Fluorinated solid electrolyte interphase enables highly reversible solid-state Li metal battery, *Sci. Adv.*, 2018, **4**, eaau9245.

98 S. Zhang, Z. Shen and Y. Lu, Research Progress of Thermal Runaway and Safety for Lithium Metal Batteries, *Acta Phys.-Chim. Sin.*, 2021, **37**, 2008065.

99 Y. Ye, W. Huang, L.-Y. Chou, J. Wan, Y. Liu, K. Liu, H. Wang, G. Zhou, Y. Yang, H. K. Lee, A. Yang, X. Xiao, X. Gao, D. T. Boyle, H. Chen, W. Zhang, S. C. Kim and Y. Cui, Ultralight and fire-extinguishing current collectors for high-energy and high-safety lithium-ion batteries, *Nat. Energy*, 2020, **5**, 786–793.

100 A. Granzow, Flame Retardation by Phosphorus Compounds, *Acc. Chem. Res.*, 1978, **11**, 177–183.

101 M. F. Rectenwald, J. R. Gaffen, A. L. Rheingold, A. B. Morgan and J. D. Protasiewicz, Phosphoryl-Rich Flame-Retardant Ions (FRIONs): Towards Safer Lithium-Ion Batteries, *Angew. Chem., Int. Ed.*, 2014, **53**, 4173–4176.

102 Y. Liu, Y. Wu, J. Zheng, Y. Wang, Z. Ju, G. Lu, O. Sheng, J. Nai, T. Liu, W. Zhang and X. Tao, Silicious nanowires enabled dendrites suppression and flame retardancy for advanced lithium metal anode, *Nano Energy*, 2021, **82**, 105723.

103 S. Kim, T. Han, J. Jeong, H. Lee, M.-H. Ryou, Y. M. Lee and A. Flame-Retardant, Composite Polymer Electrolyte for Lithium-Ion Polymer Batteries, *Electrochim. Acta*, 2017, **241**, 553–559.